

1 **Structure and environmental drivers of target resting stage of**  
2 **phytoplanktonic assemblages in Central Mediterranean Sea**

3

4 Running page head: Ecology of Mediterranean phytoplankton resting stage assemblages

5

6 Silvia Casabianca<sup>1,2\*</sup>, Samuela Capellacci<sup>1,2</sup>, Fabio Ricci<sup>1,2</sup>, Francesca Andreoni<sup>1</sup>, Tommaso7 Russo<sup>2,3</sup>, Michele Scardi<sup>2,3</sup>, Antonella Penna<sup>1,2,4</sup>

8

9 <sup>1</sup>Department of Biomolecular Sciences, University of Urbino, 61029 Urbino, Italy10 <sup>2</sup>CoNISMa, National Inter-University Consortium for Marine Sciences, 00196 Roma, Italy11 <sup>3</sup>Department of Biology, University of Rome Tor Vergata, Rome, Italy12 <sup>4</sup>IRBIM CNR, Institute for Biological Resources and Marine Biotechnology, 60125 Ancona,

13 Italy

14

15 \*Corresponding author: Silvia Casabianca, email: [silvia.casabianca@uniurb.it](mailto:silvia.casabianca@uniurb.it)

16

17

18

19 **Abstract**

20 Phytoplankton species can produce resting stages that persist in the sediments even for long

21 periods accomplishing important ecological functions. With the aim of investigating the

22 assemblage structure in relation to environmental drivers and human pressures, resting stages

23 of diatoms and dinoflagellates including HAB target taxa were analyzed in surface sediments

24 of three Mediterranean regional areas. Abundance of resting stages were determined by

25 molecular qPCR. Multivariate data analysis confirmed that the abundance of resting stage

1 assemblages seemed related to depth. Regional differences in the composition of the resting  
2 stage assemblages were evident and environmental drivers were correlated with those  
3 regional differences. Three main groups of samples were defined according to SST and depth  
4 thresholds. Samples from Northern and Central Adriatic Sea (average SST < 18°C) form the  
5 richest assemblages, both in terms of abundance and species richness, while deep samples  
6 from all the other basins (depth > 368 m) are the poorer and less diverse than those from  
7 shallower sites. Resting stage taxa contributed differently in the three groups. Diatom spores  
8 and dinoflagellate cysts were the most abundant taxa, but *Alexandrium minutum* cysts and  
9 *Ditylum brightwellii* spores also accounted for a large share of the overall inter-group  
10 distance. The structure of resting stage assemblages can be regarded as the time- and space-  
11 integrated response of a subset of phytoplankton species to the environmental conditions  
12 including the physical oceanographic dynamics that favored or prevented sedimentation of  
13 resting stages.

14

15

16 **Key words:** resting stages, assemblages, structure, sea surface temperature, depth,  
17 Mediterranean Sea, phytoplankton.

18

19

20

## 21 **1. INTRODUCTION**

22 Water column and sediments represent two most different, but linked compartments defined  
23 by specific environmental conditions where microbial assemblage structure achieves its  
24 functions (Taylor 1987, Calbet 2008).

1 Several microalgal taxa, including HAB (harmful algal bloom) species, produce resting  
2 stages that deposit onto the sea bottom forming the seed banks or assemblages which play a  
3 crucial role in maintaining microbial populations in future environments (Lennon & Jones  
4 2011). Resting stages may remain quiescent in sediments for decades or years facing  
5 environmental condition variability and potentially constituting the inoculum for future  
6 assemblages in the water column (Kremp et al. 2009, Lundholm et al. 2011, Montresor et al.  
7 2013).

8 The two major components of phytoplankton assemblage in temperate areas are  
9 dinoflagellates and diatoms. They are able to produce resting stages characterized by  
10 different morphology and eco-physiology. In particular, the diatom *Pseudo-nitzschia* spp. are  
11 generally known to do not produce resting spores, but, it is also documented that stages of  
12 non-viable dormant stages, resting cells or quiescent phase were retrieved in the sediments  
13 (Amato et al. 2005, Lundholm et al. 2010, Zhang et al. 2010, Orlova & Morozova 2009,  
14 Lelong et al. 2012). However, limited information is available on the benthic resting spores  
15 produced by *Pseudo-nitzschia* spp. (Hubbard et al. 2014).

16 The ecological role of the resting stages in coastal sediments may play a significant function  
17 for maintaining the primary production under seasonal cycling or long-term periods.  
18 Dinoflagellate and diatom resting stages may accomplish primarily in short term (seasonal)  
19 or long term (decades) survival, even if resting stage formation and deposition are long time  
20 processes in order to act in response to survival strategies (Radzikowski 2013). But, the  
21 production of asexual temporary resting stages, as dinoflagellate temporary cysts and diatom  
22 resting cells, may have a function for short-term survival stages than the resting stages  
23 (Kuwata et al. 1993, Figueroa & Bravo 2005). Under long term perspective, resting stages  
24 play an important role of resilience and recovery of the phytoplankton assemblages from  
25 abrupt environmental changes through the high genetic variability of seed banks (Kremp et

1 al. 2016). Furthermore, phytoplankton seed banks can also provide an important marine  
2 ecosystem service in terms of carbon cycling in transfer of carbon to the deep bottom as  
3 carbon sinks, and of carbon storage in coastal sediments (Ellegaard & Ribeiro 2018). Resting  
4 stages can be also passive dispersed by transport on long-distance via currents, winds,  
5 mediated by animals and humans. This allows to several phytoplankton species to outspread  
6 their distribution and colonization of new areas. In particular, for harmful species, which are  
7 associated to toxin production and bloom formation with consequent water quality  
8 degradation, this is an actual increasing trend that is often linked to aquaculture activities,  
9 ballast waters and plastic dispersion (Bolch & de Salas 2007, Perini et al. 2019, Casabianca et  
10 al. 2019).

11 Environmental variables and hydrodynamic conditions of water column can influence the  
12 resting stage assemblages in term of species composition and abundance, as well as the  
13 resting stage dynamics by coupling the benthic-pelagic components (Ribeiro & Amorim  
14 2008, Bringué et al. 2018). The environmental conditions can act primarily on the vegetative  
15 stages of many phytoplankton species in the water column. Nutrient availability, sea surface  
16 temperature, hydrodynamic conditions, irradiance and seasonal period are the main factors  
17 affecting resting stage assemblages. However, the time-lag and spatial uncertainty existing  
18 between the encystment processes from pelagic compartment and records in sediments  
19 associated to the species-specific ecophysiology makes the understanding processes of the  
20 resting stage pattern difficult (Harland et al. 2004, Anderson & Rengefors 2006).

21 The Mediterranean Sea is an oligotrophic basin highly differentiated in sub-regions based on  
22 the hydrodynamic and climatological regimes, and human coastal pressures (Reygondeau et  
23 al. 2017, Ayata et al. 2018). Those differences imply that trophic conditions and productivity  
24 are different, as well as the structure and dynamics of the phytoplankton assemblages in the  
25 water column. It is plausible to assume that also the resting stage assemblage composition

1 can retain variability traits coupled to the pelagic component (McQuoid & Godhe 2004).  
2 Areas of high productivity are mainly restricted to water close to major freshwater inputs of  
3 rivers (D'Ortenzio & Ribera d'Alcalà, 2009, Ludwig et al. 2009); but, coastal ecosystems  
4 impacted by anthropogenic nutrient input can be influenced by local hydrographic variability  
5 and conditions, which can trigger site-specific effects and patterns. Further, human activities  
6 are potent new drivers that significantly affect the functioning of coastal and off-shore marine  
7 ecosystems both in the pelagic and benthic compartments (i.e. net trawling by fishery,  
8 dredging, translocation, eutrophication, ballast water discharge and mariculture practices)  
9 (Hallegraeff 2010, Huertas et al. 2011, Penna et al. 2017). Consequently, the study of  
10 phytoplankton resting stage structure and its correlation with environmental variables and  
11 human pressures over time and space is fundamental in order to clarify the benthic-pelagic  
12 coupling and to verify the potential anthropogenic perturbations in the marine sediments,  
13 especially in coastal and open areas poor or seldom investigated as the Mediterranean Sea.  
14 The present study examined the resting stage assemblage structure from three sub-regions in  
15 the Mediterranean Sea. Through several surface sediment samples collected at various depths  
16 between November 2015 and August 2017, we estimated the abundance of main taxonomical  
17 groups of dinoflagellate and diatom, and one Raphidophyceae resting stages, including also  
18 HAB taxa, using molecular qPCR (quantitative polymerase chain reaction) assay in relation  
19 to several environmental variables and human impact. Statistical analyses provided clear  
20 insights into the relationships between resting stage assemblages and drivers in the marine  
21 ecosystems surrounding Mediterranean coastlines.

22

## 23 **2. MATERIALS AND METHODS**

### 24 **2.1. Sediment sampling**

1 A total of 94 surface sediments were collected at several sampling stations in the marine sub-  
2 regions of the Mediterranean Sea, such as Adriatic, Ionian and Tyrrhenian Sea (Table S1)  
3 during different cruises operated by CNR (Consiglio Nazionale delle Ricerche) - CoNISMa  
4 (Consorzio Nazionale Interuniversitario per le Scienze del Mare) in 2015-2017. All samples  
5 were collected at coastal and off-shore areas, while accumulation sites, such as harbours or  
6 bays, were not sampled. Sediment samples were collected by means of a gravity Van Veen  
7 grab sampler operated on board of Minerva Uno vessel owned by CNR. Surface samples  
8 were harvested at depths ranging from 1 to 1018 m. Three samples were collected per each  
9 sampling station. The surface portion (1 cm) of each sample was placed in sterile tubes using  
10 sterile spatula and kept in the dark at +4°C till processed.

11

## 12 **2.2. Microalgal cultures**

13 Target species of *Chaetoceros socialis* CBA22, *Ditylum brightwellii* CBA2, *Skeletonema*  
14 *marinoi* CBA4, *Thalassiosira* sp. CBA3, *Scrippsiella trochoidea* CBA3, were isolated by  
15 micropipetting from net surface seawater samples collected at 3000 m off the NW Adriatic  
16 coast at Foglia (43°56.85'N, 12°56.10'E) and Metauro (43°50.65'N, 13°03.83'E) stations.  
17 Light microscopy observation and isolation of living cells were carried out using an Axiovert  
18 40 CFL, Zeiss at 200x and 400x magnifications. Strains of *A. tamarense* VGO1042,  
19 *Gymnodinium impudicum* GY6V, *Heterocapsa triquetra* RCC4813 and *Heterosigma*  
20 *akashiwo* HA2V were obtained from algal collection of Instituto Español de Oceanografía  
21 (IEO, Spain). Bacillariophyceae monoclonal cultures were maintained in f/2 medium  
22 (Guillard 1975) at  $16 \pm 1$  °C, while various Dinophyceae and Raphidophyceae strains were  
23 maintained in different media (Table S2) at  $23 \pm 1$  °C. Light was provided at an irradiance of  
24  $100 \mu\text{E m}^{-2} \text{s}^{-1}$  on a standard 14:10 h light/dark cycle. Microalgal cultured subsamples  
25 containing  $1.0 \times 10^5$  cells were collected between the 6<sup>th</sup> and 7<sup>th</sup> day during the exponential

1 growth phase and centrifuged at 4000 rpm for 15 min. Pellets were stored at  $-80^{\circ}\text{C}$  until  
2 molecular analyses.

3

### 4 **2.3. Molecular analyses**

5 In order to ensure that only resting stages survived in the sediments, all sediment samples  
6 were stored in the dark at  $4^{\circ}\text{C}$  for several weeks and treated to obtain purified phytoplankton  
7 resting stage pellets. Briefly, wet subsamples (about 5 g) were suspended in filtered seawater  
8 ( $0.45\ \mu\text{m}$ ) and incubated in an ultrasonic bath (Bandelin, Germany) for 2 min at room  
9 temperature to separate resting stages from sediment particles. The suspension was then  
10 sieved through a steel mesh (Endecotts, UK) using 100 and  $20\ \mu\text{m}$  size fractionation, washed  
11 with seawater. Resting stages were separated from detrital material by Bolch's (1997) density  
12 gradient method, using sodium polytungstate solution (SPT) and a centrifugation step. The  
13 interface containing resting stages was placed into a new tube, filled with filtered seawater,  
14 and centrifuged twice to recover resting stage material (for details see Perini et al. 2019).

15 In order to remove the potential DNA debris from dead vegetative cells, resting stage pellets  
16 were suspended in  $500\ \mu\text{l}$  of distilled water, incubated at  $+75^{\circ}\text{C}$  for 10 min and centrifuged  
17 at 4000 rpm for 7 min following the protocol developed by Kim et al. (2016). Genomic DNA  
18 extraction from both cultured microalgal cell and resting stage pellets was performed using  
19 DNeasy PowerSoil Kit (Qiagen, Hilden, Germany), according to the manufacturer's  
20 instructions. Finally, DNA was quantified using a Qubit fluorometer with a Quant-iT dsDNA  
21 HS assay Kit (Invitrogen, Carlsbad, CA, USA) and stored at  $-20^{\circ}\text{C}$  until molecular analyses.

22 In the present study, the sediment samples were analysed for the quantification of a total of  
23 17 diatom and dinoflagellate taxa by molecular qPCR assay (Table S3). Seven new taxon-  
24 specific primers for *C. socialis*, *D. brightwellii*, *Skeletonema* spp, *Thalassiosira* spp.,  
25 *Gymnodinium* spp., *H. triquetra* and *S. trochoidea* species complex were designed on LSU

1 (large subunit) or 5.8S-ITS (5.8S subunit and internal transcribed spacers ITS1 and ITS2)  
2 rDNA gene sequences available from GenBank using Primer-BLAST (Ye et al. 2012).  
3 Multiple sequence alignments were carried out using CLUSTALX2 v. 2.0 (Larkin et al.  
4 2007). The specificity of the new primers was tested *in silico* using BLAST (Basic Local  
5 Alignment Search Tool) and by qPCR with genomic DNA from non-target species (Table  
6 S2). Moreover, primers for the quantification of Dinophyceae and Bacillariophyceae were  
7 used as described in Casabianca et al. (2019). The qPCR quantifications of other 8  
8 phytoplankton taxa as *A. minutum*, *A. pacificum*, *G. spinifera*, *L. polyedrum*, *P. reticulatum*  
9 (*Perini et al. 2019*), and *A. tamarense/A. mediterraneum*, *Pseudo-nitzschia* spp. (*Penna et al.*  
10 *2007*), and *H. akashiwo* (*Yuan et al. 2015*) were also performed. The qPCR reactions were  
11 done in a final volume of 25  $\mu$ l using the Hot-Rescue Real Time PCR Kit-SG (Diatheva,  
12 Fano, Italy), 0.5 U of Hot-Rescue Taq DNA polymerase and 1  $\mu$ l undiluted and 1:10 diluted  
13 DNA template. Primer and MgCl<sub>2</sub> concentrations, melting temperatures, amplicon sizes and  
14 rDNA target region are shown in Table S3. The thermal cycling conditions consisted of 10  
15 min at 95 °C, followed by 40 cycles at 95 °C for 15 s and 60 °C for 1 min. All amplification  
16 reactions were carried out in a StepOne Real-Time PCR System (Applied Biosystems, Foster  
17 City, CA, USA). Standard curves were included in each PCR reaction. All samples were run  
18 with three biological replicates, each of which was run with two technical replicates.  
19 Standard curves for the seven new primer sets were constructed using a 6-point tenfold  
20 dilution series of purified rDNA PCR products (from 2 to  $1.0 \times 10^6$  copies) generated from  
21 DNA of the target species as described in *Perini et al. (2019)*. The *A. tamarense* CNRATAA1  
22 plasmid was used for the *A. tamarense/A. mediterraneum* standard curve generation.  
23 Standard curves for quantification of the remaining target taxa were previously described  
24 (*Penna et al. 2013*, *Yuan et al. 2015*, *Perini et al. 2019*). In particular, for the quantification of  
25 Dinophyceae and Bacillariophyceae, the cellular standard curves were obtained by mixing



1 purified DNAs from 20 different monoclonal cultures of microalgae belonging to the two  
2 classes. Based on the assumption that the number of copies of SSU rDNA is proportional to  
3 the biomass of the species, a variety of class size of dinoflagellates and diatoms with different  
4 range of copy number were used (Godhe et al., 2008, Penna & Galluzzi, 2013, Perini et al.  
5 2019, Gong & Marchetti 2019). In the present study, in order to reduce the potential rDNA  
6 copy number variability, the cellular standard curves were constructed using a mix of  
7 cultured strain cells of dinoflagellates and diatoms (Casabianca et al. 2019). By interpolating  
8 the Ct (threshold cycle) determined experimentally on standard curves, the copy number of  
9 both cultured strains and purified resting stages from sediment samples were obtained.  
10 Multiplication by the dilution factor allowed calculation of the total number of copies g<sup>-1</sup> of  
11 dry weight (d.w.) of sediment sample. This value was then divided by the number of copies  
12 cell<sup>-1</sup> obtained from cultured strains to obtain the resting stages number g<sup>-1</sup> of d.w.  
13 Acquisition of qPCR data and subsequent analyses were carried out using StepOne software  
14 v. 2.3 (Applied Biosystems). A dissociation curve was generated after each amplification run  
15 to check for amplicon specificity and primer dimers. The automatically generated standard  
16 curves were accepted when the slope was between 3.59 and 3.32 (90 – 100% efficiency) and  
17 the determination coefficient (r<sup>2</sup>) was at least 0.99. Amplification efficiency was calculated as  
18  $(10^{(-1/\text{slope})} - 1) \times 100$ .  
19 Statistical analyses were performed with non-parametric Spearman correlation test using  
20 PAST ver. 3.2 (Hammer et al. 2001).

21

#### 22 **2.4. Cultured strain sequencing**

23 The strains of *Scrippsiella* spp. and *Chaetoceros* spp. obtained in this study were sequenced  
24 to confirm the species-specific taxonomical assignment by ITS-5.8S and LSU rDNA  
25 sequence alignment. The sequences of ribosomal genes obtained from new cultured isolates

1 were deposited in the NCBI (National Center for Biotechnology Information) database. The  
2 ITS-5.8S region of the rDNA was amplified and sequenced using the universal primer ITSA  
3 and ITSB (Adachi et al. 1994). The LSU rDNA was amplified and sequenced using D1R and  
4 D2C primers (Scholin et al. 1994) targeting the D1-D2 region. The PCR reaction for the ITS-  
5 5.8S rDNA and LSU rDNA was as follows: tubes contained 25  $\mu$ l of 1X reaction buffer (Hot  
6 Start Taq DNA Polymerase 5U/ $\mu$ l, Biotechrabbit GmbH, Germany), 2.5 mM of  $MgCl_2$ ,  
7 0.75X PCR Enhancer, 200  $\mu$ M of dNTPs, 200 nM or 400 nM of each primer for ITS and  
8 LSU, respectively, 1U Taq DNA Polymerase and 0.5–1 ng of DNA template. PCR thermal  
9 cycling conditions were the same as reported in Pugliese et al. (2017). All amplified PCR  
10 products were purified using the MinElute Gel Extraction Kit (Qiagen), and the products  
11 were directly sequenced with the ABI PRISM BigDye Terminator Cycle Sequencing Kit v.  
12 1.1 on the ABI 310 Genetic Analyzer (Applied Biosystem, Foster City, CA, USA). Standard  
13 thermal cycling conditions were used for both templates setting the annealing temperature  
14 according to the template (60 °C and 50 °C for ITS and LSU PCR specific primers,  
15 respectively). Difficult templates and repeated regions were solved increasing initial  
16 denaturation time and modifying thermal cycling condition as follows: 40 cycles of  
17 denaturation at 96 °C for 10 s and annealing/extension at 50 °C for 4 min. The *Scrippsiella*  
18 spp. and *Chaetoceros* spp. ITS-5.8S and LSU sequences were aligned *in silico* using BLAST  
19 database.

20

## 21 **2.5. Statistical methods**

22 The resting stage assemblage data set included the abundances of 17 taxa (Table S3) as  
23 number of cysts or spores  $g^{-1}$  d.w. sediment at 94 sampling stations (Table S1). Moreover, at  
24 each sampling station, depth was recorded, whereas the values for other 20 environmental  
25 variables were retrieved as the average value in a 1 m radius from GIS (Geographic

1 Information System) raster layers with a pixel size of  $\frac{1}{4}$  minute (Table S4). Bathymetric data  
2 were obtained from EMODNet Hydrography Portal (2013). Environmental variables were  
3 not selected among those available at adequate spatial scale on the basis of potential causal  
4 relationships with the structure of the resting stage assemblages, as those relationships are  
5 obviously unknown. Moreover, all the selected environmental variables express properties  
6 that are steady state or still meaningful when averaged in time. Needless to say, physical  
7 properties of the water column or patterns in currents would have been useful from a  
8 theoretical viewpoint, but they were not available at our study scale. As for the amount of  
9 fishing effort deployed by the fleet of Italian trawlers with length-over-all (LOA) larger than  
10 15 m, it was estimated as total fishing time (in hours) in the year 2016, with respect to a 0.01  
11 degree square grid. The activity of 1170 trawlers were reconstructed from a Vessel  
12 Monitoring System (VMS) database provided, within the framework of Data Collection in  
13 the Fisheries Sector ([https://ec.europa.eu/fisheries/cfp/fishing\\_rules/data\\_collection\\_en](https://ec.europa.eu/fisheries/cfp/fishing_rules/data_collection_en)),  
14 from the National Ministry of Agricultural Food, Forestry, and Tourism Policies. VMS is the  
15 most important and reliable remote tracking device used worldwide (Amoroso et al. 2018) to  
16 monitor and control fishing activities. Although VMS is mandatory only for large fishing  
17 vessels, it was repeatedly demonstrated that it is able to capture the largest portion of pressure  
18 and related impacts exerted by the fleets (Russo et al. 2016). VMS data were processed using  
19 the VMSbase platform, which implements standard procedures for cleaning, interpolation  
20 and identification of fishing set positions (Russo et al. 2014, Eigaard et al. 2017). Other  
21 activities (e.g. steaming or in harbor parking) were excluded. All GIS activities were  
22 performed under QGIS 2.16.2 (QGIS Development Team, 2015).

23 Resting stage abundances were log-transformed as  $x' = \log_{10}(x+1)$  before any statistical  
24 analysis in order to reduce the heterogeneity in the available values, which spanned over  
25 more than 4 orders of magnitude, and to normalize as far as possible their distributions.

1 Redundancy Analysis (RDA) (Rao 1964, Wollenberg 1977) was selected as the best suited  
2 ordination technique to explore the overall relationships between resting stage assemblages  
3 and environmental and biotic variables. In fact, it aims at restricting the number of linear  
4 combinations of explanatory (environmental) variables that are related to some dependent  
5 (biotic) variables to some small rank and it can be regarded as a Principal Component  
6 Analysis performed on the projections of the latter variables on the space spanned by the  
7 former ones. RDA allowed permutation-based tests for independence between environmental  
8 and biotic variables and for significance of each canonical axis. RDA and all related tests  
9 were performed using the *rda* function in the *vegan* package (Oksanen et al. 2018) under the  
10 R 3.51 statistical computing environment (R Core Team 2018). In order to avoid problems  
11 related to collinearity, only environmental variables with a Variance Inflation Ratio (VIR)  
12 smaller than 10 according to the *vir* function from the same package were included in the  
13 analysis. As RDA can be regarded as an extension of Principal Component Analysis, it  
14 operates in a Euclidean space and therefore Euclidean distances were also used in subsequent  
15 analyses.

16 A Multivariate Regression Tree (MRT) (De'ath 2002) was trained using the *mvpart* function  
17 of the *mvpart* 1.6.2 package (De'ath 2014). The MRT was used to split the set of resting  
18 stages samples into the most homogeneous subsets that can be obtained on the basis of  
19 threshold values for selected environmental variables. The MRT was based on Euclidean  
20 distances and 5-fold cross-validation was repeated 100 time. The selection of the most  
21 parsimonious tree was carried out using the *plotcp* function of the same package. As any  
22 other tree-based Machine Learning classification technique, MRTs are not affected by  
23 collinearity, and therefore, all the available variables have been included in the training data  
24 set.

1 The role played by each taxon in determining the differences between the groups of samples  
2 defined by the MRT was analyzed by means of the Similarity Percentage (SIMPER) on  
3 Euclidean distances (Clarke 1993). SIMPER, as well as uni- and bivariate analyses, were  
4 performed using PAST (Hammer et al. 2001).

5

### 6 **3. RESULTS**

#### 7 **3.1. Sequencing analyses and primer specificity**

8 The rDNA gene sequences of *Chaetoceros* spp. and *Scrippsiella* spp. strains were identified  
9 based on sequence similarity using BLAST. One strain was identified as *C. socialis* CBA22  
10 (GenBank accession no. MK881016). The three strains CBA1S, CBA2 and CBA3 of  
11 *Scrippsiella* were identified as *S. trochoidea* species complex including *S. acuminata*  
12 (GenBank accession no. MK881019), *S. erinaceus* (GenBank accession no. MK881020), *S.*  
13 *trochoidea* var. *aciculifera* (GenBank accession no. MK881021) due to the high level of  
14 similarity among ribosomal DNA sequences (100 – 99% of similarity). Therefore, in the  
15 present study, *S. trochoidea* species complex was investigated including other potentially  
16 closely related species (see also Gottschling et al. 2005, Lee et al. 2018).

17 The species-specificity of seven new primers designed to target *C. socialis*, *D. brightwellii*,  
18 *Skeletonema* spp., *Thalassiosira* spp., *Gymnodinium* spp., *H. triquetra* and *S. trochoidea*  
19 species complex was tested *in silico* using BLAST. The results indicated that primers were  
20 highly specific. Primer species-specificity was also assayed using DNAs of other  
21 phytoplankton species (Table S2). Negative amplifications were obtained confirming the  
22 species-specificity of the primers (data not shown).

23

#### 24 **3.2. Standard curves and abundance of resting stages in sediment samples**

1 Standard curves used to calculate the number of copies in each reaction (Table S5) showed a  
2 PCR efficiency from 90 to 100%, a linear relationship over a range of 6 orders of magnitude  
3 ( $r^2 = 0.99$ ) and a quantification limit of two copies per PCR reaction. The reproducibility of  
4 qPCR assay was analyzed both, as  $CV_{Ct}$  (coefficient of variation of cycle threshold) and  $CV_{Cn}$   
5 (coefficient of variation of copy number). The  $CV_{Ct}$  mean inter-assay variability ranged from  
6 0.5 to 1.4% ( $1.0 \times 10^6 - 2$  copies), while, the  $CV_{Cn}$  mean values ranged from 9.9% to 25.5%  
7 ( $1.0 \times 10^6 - 2$  copies).

8 Accurate resting stage quantification of Dinophyceae and Bacillariophyceae and other target  
9 phytoplankton taxa was performed by qPCR assay in surface sediment samples. The  
10 maximum abundance of dinoflagellate cysts ( $9878 \pm 467$  cysts  $g^{-1}$  d.w.) was observed at 22 m  
11 of depth at MS16\_III\_147 sampling station, a sampling site about 4 miles south of the Po  
12 Delta (Adriatic Sea) during the third campaign of the 2016. The maximum diatom spore  
13 abundance ( $34329 \pm 4308$  spores  $g^{-1}$  d.w.) was found at 41 m of depth at MS17\_I\_111\_C  
14 station in Tyrrhenian Sea during the first campaign of the 2017. The lowest values of both  
15 taxa, were found at MS16\_II\_77, Ionian Sea, in the second campaign of the 2016 and at  
16 MS17\_II\_035\_C R1, Strait of Sicily, in the second campaign of the 2017 at 930 and 418 m of  
17 depth, for Dinophyceae and Bacillariophyceae, respectively. Moreover, no diatom spores  
18 were found in three samples collected in the Ionian Sea (at 415, 766 and 930 m depth) and in  
19 three samples from Tyrrhenian Sea (at 440, 446 and 495 m depth) (Fig. 1). The abundance of  
20 resting stages decreased with depth increasing based on significant negative correlation  
21 obtained between depth and the two class' abundance ( $n = 94$ , Spearman's  $r_s = -0.73$ ,  $p \ll$   
22  $0.001$  and Spearman's  $r_s = -0.60$ ,  $p \ll 0.001$  for Dinophyceae and Bacillariophyceae resting  
23 stages, respectively). Further, higher resting stages abundance of one class was directly  
24 linked to an increased abundance of the other (Fig. 2) based on significant positive  
25 correlation ( $n = 94$ , Spearman's  $r_s = 0.86$ ,  $p \ll 0.001$ ) found between Dinophyceae and

1 Bacillariophyceae abundance. Further, in the Adriatic Sea sediments, the diatom *D.*  
2 *brightwellii* resting stages were the most abundant with  $4911 \pm 475$  spores  $g^{-1}$  d.w. at 33 m  
3 depth at MS16\_III\_165 followed by the highest cyst number of *A. minutum* ( $1032 \pm 77$  cysts  
4  $g^{-1}$  d.w.) at 35 m depth MS15\_55 station (Fig. 3a). In the Ionian Sea, the dinoflagellate  
5 *Gymnodinium* spp. cysts were the most abundant ( $174 \pm 14$  cysts  $g^{-1}$  d.w.) at 188 m depth at  
6 MS\_152 station followed by the diatom *C. socialis* spore abundance ( $43 \pm 5$  spore  $g^{-1}$  d.w.) at  
7 130 m depth at MS17\_II\_041\_CR1 (Fig. 3b). Finally, in the Tyrrhenian Sea, the diatom  
8 *Pseudo-nitzschia* spp. presumably non-viable dormant stages were the most abundant with  
9 the presence of  $297 \pm 11$  spores  $g^{-1}$  d.w. at 41 m depth at MS17\_I\_111\_C followed by *C.*  
10 *socialis* spores ( $149 \pm 11$  spore  $g^{-1}$  d.w.) at 127 m at MS17\_I\_84\_CR1 (Fig. 3c). Among the  
11 toxic producing taxa, *Pseudo-nitzschia* spp. non-viable dormant stages and *L. polyedrum*  
12 resting stages were found the most frequent in the range of 77-76% of presence in the 94  
13 sediment samples analyzed. Indeed, *A. minutum* and *P. reticulatum* were retrieved in the  
14 highest abundance in Adriatic Sea both at 35 m with  $1032 \pm 77$  and  $796 \pm 87$  cysts  $g^{-1}$  d.w.,  
15 respectively. The Raphidophyceae *H. akashiwo* was found in a single Tyrrhenian Sea  
16 sediment sample at 127 m depth at MS17\_I\_84\_CR1, with  $8 \pm 1$  cysts  $g^{-1}$  d.w. (data not  
17 shown).

18

### 19 3.3. Resting stage assemblage analysis

20 The resting stage assemblage included a very heterogeneous subset of the taxa that can be  
21 found in the water column throughout the seasonal successional cycle. Taxa in this subset  
22 differed by 3-4 orders of magnitude in their abundances.

23 While relationships between sampling depth and the abundance of dinoflagellate cysts and  
24 diatom spores had been already detected, an overall dependence of the resting stage  
25 assemblage on the environmental variables was also detected. A Redundancy Analysis

1 (RDA) was performed, taking into account resting stage abundances of 17 taxa and 9  
2 environmental variables out of the available 21 (see short names with an asterisk in Table S4,  
3 selected among). In order to avoid problems related to strong collinearity, environmental  
4 variables with a VIF larger than 10 were filtered out and excluded from the RDA, then the  
5 null hypothesis of independence between biotic and abiotic data subsets was rejected on the  
6 basis of the ANOVA-like permutation test ( $p = 0.001$  with 999 permutations) associated to  
7 the RDA. According to the same procedure, only the first two canonical axes were found to  
8 be significant ( $p = 0.001$  and  $p=0.014$ , respectively, with 999 permutations), but they  
9 accounted for a very large share of variance, i.e. 49.88% (RDA1 44.27% and RDA2 5.59%)  
10 (Fig. S1). The RDA allowed visualizing the differences in composition of resting stage  
11 assemblages in the three subregional Seas, i.e. Adriatic, Ionian and Tyrrhenian Seas and their  
12 association with resting stages taxa and environmental variables. All the resting stages were  
13 more frequent in the Adriatic Sea, whose resting stages assemblages were also found to be  
14 more abundant. Fishing pressure (fishing in the ordination) was higher in that region than in  
15 the others, which were associated to higher values for all the remaining variables, with the  
16 only exceptions of seafloor temperature (bottemp, higher because of the limited depth of the  
17 Adriatic Sea) and human impact (i.e. impact, as defined by Halpern et al., 2008) that seems  
18 independent of differences between basins. While the RDA ordination seemed consistent  
19 with the spatial distribution of resting stages, abundances of resting stages were not  
20 homogeneous among Adriatic, Ionian and Tyrrhenian Seas, as shown by a Kruskal-Wallis  
21 test ( $H = 22.87$ ,  $p < 0.001$ ). A significantly lower median abundance of resting stages was  
22 also found in the Ionian samples relative to the Adriatic ones (post-hoc Mann Whitney test  
23 with Bonferroni correction,  $U = 254$ ,  $p < 0.001$ ).

24 While grouping samples according to the basin where they were collected, i.e. according to  
25 the most natural partition, allowed to point out some general relationships thanks to the RDA,



1 a more effective partition of the data set was obtained thanks to a Multivariate Regression  
2 Tree, which was mainly driven by SST and depth and only partly reflected subregional  
3 differences between basins. In fact, the MRT allowed to find the most parsimonious optimal  
4 partition of the resting stage data set, as well as the environmental variables and the cut-off  
5 values that defined that partition. As it was based on Euclidean distances computed from log-  
6 transformed abundances, it operated in the same data space as the RDA.

7 The analysis of the cross-validation error based on 100 iterations (Fig. S2) showed that the  
8 minimum value (0.5998) was obtained for a MRT with three leaves. This was also the most  
9 parsimonious tree within one standard error from the minimum value of the cross-validation  
10 error and therefore it was selected as the optimal solution also according to Breiman et al.  
11 (1984) (Fig. 4). The first split was based on the average SST, with a cut-off value of 18.57  
12 °C, and generated a first leaf, including 26 sediment samples from cooler waters, and second  
13 split was based on depth. The latter split was associated to a cut-off value of 368 m and the  
14 two leaves that were generated included 53 shallower sediment samples and 15 deeper ones,  
15 respectively. Leaves in the MRT were labelled with symbols (gray circle, black triangle and  
16 white square) which have been consistently used as reference.

17 While the average within-group Euclidean distance was 6.303 when samples were grouped  
18 by subregional sea, the groups obtained from the MRT leaves were more homogenous, with a  
19 5.050 average within-group Euclidean distance. The difference was highly significant ( $t =$   
20 15.047,  $p \ll 0.001$ ) and showed that the partition generated by the MRT fitted the resting  
21 stage data much better than the one based on a strictly geographical criterion, although the  
22 latter can be regarded as a proxy for several relevant ecological and oceanographic features.

23 Each leaf in the MRT was associated to the average composition of the subset of resting stage  
24 samples it represents as shown in the small bar diagrams. While the three average  
25 assemblages clearly differed from each other, they did not allow an easy comparison of their

1 composition and the only feature that could be easily grasped was the major role played by  
2 the taxa in the first two bars from the left, i.e. dinoflagellate cysts and diatom spores,  
3 respectively. These taxa were dominant in all the leaves, although to a lesser extent in the  
4 leftmost one, including 15 sediment samples. A more complete analysis of the average  
5 resting stage assemblages obtained from the MRT was carried out by means of a SIMPER  
6 procedure (Table 1). The various taxa were ranked according to their contribution to the  
7 average Euclidean distance between the resting stage assemblages associated to the three  
8 leaves of the MRT. Distances were computed, as in the previous analyses, based on  
9  $\log_{10}(x+1)$  transformed abundances (cysts or spores  $\text{g}^{-1}$  d.w.). For each taxon, from left to  
10 right, the average distance between the groups of samples in the MRT leaves, the percent  
11 contribution to the overall average distance and the cumulative percent contribution to the  
12 overall distance were shown. The log-transformed average abundance in the assemblages  
13 associated to each leaf, were represented as a horizontal bar and as a number. The three  
14 rightmost columns, showing the average structure of the resting stage assemblages, can be  
15 associated to the corresponding leaf in the MRT by means of the symbol or of the cut-off  
16 values for temperature (SST) and depth.

17 As previously mentioned, the two broadest taxa (dinoflagellate cysts and diatom spores)  
18 played important roles, but also two species provided comparable contributions to the overall  
19 distance between resting stage assemblages, such as *A. minutum* cysts and *D. brightwellii*  
20 spores. Both species contributed more than 20% of the overall distance and together with the  
21 two broadest taxa accounted for more than 50% of the overall distance between the samples.  
22 Six more taxa, at species or genus level, accounted for an additional 45% of the overall  
23 distance, thus leaving less than 5% of the overall distance to the seven least abundant taxa.  
24 The general pattern that emerged from the MRT and SIMPER analysis of its leaves showed  
25 that the average abundance of resting stages was maximum in samples collected at sites with

1 average SST lower than 18.57 °C, while intermediate abundances were found at warmer  
2 stations whose depth was less than 368 m. Deeper stations whose average SST was higher  
3 than 18.57 °C had the poorest resting stage assemblages, although dinoflagellate cysts and  
4 diatom spores still played the most important role. The abundance of all taxa was  
5 monotonically decreasing from right to left in the MRT and from left to right in Table 1, with  
6 the only exception of the *C. socialis* spores, which are slightly more abundant in the deepest  
7 subset of warmer samples than in the shallower ones.

8 In the Mediterranean Sea, the spatial distribution of the sediment samples was assigned to  
9 each leaf of the MRT (Fig. 5). Different shades of gray show the distribution of the variables,  
10 which were selected for the MRT splits, as average SST and depth. Marine regions in white  
11 were those where the average SST was lower than 18.57 °C, and included northern and  
12 Central Adriatic Sea in addition to the western Ligurian Sea, the northern western  
13 Mediterranean and two regions eastern and western of the Strait of Bonifacio where the  
14 effects of the mistral frequently cool down the upper layer of the water column. However, no  
15 sediment samples were available in the latter regions, while several samples (n = 26) were  
16 collected at shallow sites with average SST values below 18.57 °C in coastal Adriatic regions  
17 at North of 41°, and all of them belonged to the first leaf of the MRT. This grouping included  
18 the highest abundances of resting stages were associated. The average depth of this group of  
19 sampling stations was 36 m. All the remaining samples belonged to one of the two leaves  
20 generated by the second split in the MRT, which was based on depth, with 368 m as cut-off  
21 value. The shallower region was shown in light gray and included 53 sampling stations,  
22 scattered along the Ionian and Tyrrhenian neritic waters. In few cases, water depth was down  
23 to the upper part of the continental slope, but with an average depth of 130 m. The deepest  
24 stations (n = 15), with an average depth of 641 m, were located in most cases very close to

1 the boundary between the shallower waters and the deeper region that stretches beyond the  
2 368 m isobaths, down to the deepest part of the Ionian and Tyrrhenian basins.

3

#### 4 **4. DISCUSSION**

5 In the present study, target phytoplankton taxa producing resting stages were studied based  
6 on their higher presence and abundance, and also for their bloom formation in the  
7 Mediterranean seed banks and surface water, respectively. Among phytoplankton species  
8 forming resting stages, target HAB taxa were also investigated as they could represent a  
9 threatening for new blooms origination especially at coastal areas. These species are known  
10 to be widespread and abundant in the Mediterranean sampled areas (Rubino et al. 2009,  
11 Anglés et al. 2010, Satta et al. 2010, Penna et al. 2010, Montresor et al. 2013, Piredda et al.  
12 2017, Perini et al. 2019).

13 Due to the huge extension of the Mediterranean bottom, the number of known and unknown  
14 taxa, and the relative amount of molecular primers to be used in qPCR assay, it is not yet  
15 feasible to quantify all diversity of resting stage taxa present in the sediments. As far to date,  
16 few molecular data are present to inform us about the diversity of resting stages produced by  
17 diatoms or dinoflagellates in the Mediterranean Sea (Piredda et al. 2017, Perini et al. 2019).  
18 So, it is challenge starting to explore the diversity of resting stage assemblages in this basin in  
19 order to know taxa richness and structure of resting stage assemblages in relation to  
20 environmental variables and human impact. Regional seas were sampled at coastal and off-  
21 shore areas in the Mediterranean basin. The molecular analysis of target resting stage of  
22 phytoplankton assemblages in marine sediments of the Central Mediterranean Sea was  
23 carried out by using more sensitive and specific qPCR assay than traditional microscopy.

24 Among the molecular quantified resting stages, presumably non-viable dormant stages of  
25 *Pseudo-nitzschia* were found in the majority of samples. However, it is still known that

1 formation of resting stages by *Pseudo-nitzschia* has not been reported (Piredda et al. 2017).  
2 However, it was hypothesized that *Pseudo-nitzschia* spp. may have a quiescent phase either  
3 in the water column or in the sediment, during which cell division, and therefore size  
4 reduction, are markedly reduced (Amato et al. 2005). In support of this hypothesis, some  
5 authors documented the presence of *Pseudo-nitzschia* spp. preserved valves in sediments  
6 (Parsons & Dortch 2002, Abrantes et al. 2007, Lundholm et al. 2010). In particular, preserved  
7 valves of *Pseudo-nitzschia* spp. and intact cells of *P. pungens* with cell content in the core  
8 sediments were found and presumably these could be non-viable dormant stages.

9 The molecular approach has been successfully applied mainly for the quantification of target  
10 harmful microalgal species in different environmental matrices allowing a rapid examinations  
11 of field samples. High-throughput qPCR platforms permit the simultaneous processing of a  
12 large number of samples, significantly decreasing processing time compared to microscopic  
13 procedures that also require high level of taxonomical expertise (Fitzpatrick et al. 2010,  
14 Perini et al. 2011, Casabianca et al. 2013, Penna et al. 2013, Casabianca et al. 2014, Kon et  
15 al. 2017).

16 In the present study, the decreasing of resting stage abundances of dinoflagellates and  
17 diatoms, which are considered the two dominant groups in marine phytoplankton, in relation  
18 to depth down to about 1000 m was a clear evidence emerging from statistical analyses.  
19 Resting stage abundance was found to be higher in shallower sites than in deeper ones, with  
20 larger amounts of resting stages produced by diatoms rather than by dinoflagellates. Resting  
21 stages have different sinking rates in the water column based on their peculiar biological and  
22 physical properties. Dinoflagellate cysts and diatom spores retain sinking rates between 6 –  
23 11 m d<sup>-1</sup> and 0.57–16 m d<sup>-1</sup>, respectively (Anderson et al. 1985, French & Hargraves 1980).  
24 However, resting spores can also aggregate passively in marine snow with a sinking rate of  
25 43 – 95 m d<sup>-1</sup> (Shanks & Trent 1980), which is faster than that of individual resting stages.

1 Therefore, cysts and spores reach the sea floor with different sinking times. In the present  
2 study, we assessed that spores and cysts likely sink down to the deepest station (1018 m) in a  
3 lapse of time ranging between 15 days and 4 months.

4 Furthermore, seawater trophic conditions can influence the structure of phytoplankton  
5 assemblages in term of species abundance, composition and succession (Hernández-Fariñas  
6 et al. 2014, Otero et al. 2018) and related formation of resting stages. Major phytoplankton  
7 groups often differ in average functional trait values, thus implying diverse performance and  
8 fitness under environmental conditions (Barton et al. 2013). Diatoms, often of small size,  
9 seem to follow the r-strategy in mixing waters characterized by high nutrient concentrations.

10 They are typically dominant in coastal waters that receive riverine input as well as open  
11 waters in favourable upwelling conditions. Instead, dinoflagellates are expected to be more  
12 abundant in calm, confined and warm coastal waters (Finkel et al. 2010, Mutshinda et al.  
13 2016). These trophic and hydrodynamic conditions are found in the Mediterranean areas  
14 where sampling activities were carried out (Valbi et al. 2019). Resting diatom spore  
15 abundance was higher than dinoflagellate cyst amount in all sampled areas with the highest  
16 abundance in the Adriatic Sea. This latter aspect could be related to the mesotrophic  
17 conditions, especially in the north and central portion of the basin, where it receives major  
18 riverine input. This environment is often favourable for diatom blooms which can sustain  
19 encystment processes in the water column. Further, high spore density was found below 20 m  
20 reaching the highest values ( $10 - 27 \times 10^4$  cysts  $g^{-1}$  d.w.) from 31 to 65 m. The diatom *D.*  
21 *brightwellii* was the most abundant species followed by *C. socialis* and *Thalassiosira* spp. In  
22 the other two basins considered, i.e. Ionian and Tyrrhenian, spores were found in lower  
23 abundances, although in deeper stations in comparison with Adriatic Sea. In general,  
24 dinoflagellate cysts were found in lower abundance in all sampled areas (below  $10^4$  cysts  $g^{-1}$   
25 d.w.) and highest amounts were found below 30 m. Again, the Adriatic Sea resulted the most

1 productive area for cyst deposition on surface bottom. Among the dinoflagellate cyst taxa, the  
2 potentially harmful species, as *A. minutum* and *Gymnodinium* spp., were found to be the most  
3 abundant ones in the range of  $10^3 - 10^2$  cysts  $g^{-1}$  d.w. The higher abundance of resting stages  
4 found mostly below 20 m can be likely associated to a lesser disturbance effect by wave  
5 motion or anthropic activities (shipping, harbours, tourism, infrastructures, riverine input and  
6 sewage). However, shallower stations presenting higher resting stage abundance provided a  
7 seafloor that can be reached very quickly by resting stages and may present more  
8 advantageous environmental conditions to their survival (Bastianini et al. 2016).

9 Multivariate data analyses confirmed that the abundance of the resting stage assemblages  
10 seemed related to depth, as it was consistently higher in shallower samples. While this  
11 general pattern is very clear even when single taxa were considered, differences in  
12 assemblage structure showed that depth was not the only variable affecting distribution and  
13 abundance of the resting stages.

14 The ordination obtained from the RDA, with almost 50% of the total variance explained by  
15 the first two axes, showed regional differences in the composition of the resting stage  
16 assemblages, but it also showed how environmental drivers were related with those regional  
17 differences. Permutation-based test confirmed that this overall relationship as well as the two  
18 above-mentioned canonical axes were significantly different from those expected by chance  
19 and therefore, the dependence of the resting stage assemblages from the environmental  
20 conditions can be regarded as something more than a simple hypothesis.

21 However, while RDA allowed analyzing the relationships between the resting stages and  
22 explanatory environmental variables, the latter were not independent from each other and not  
23 all of them were necessarily relevant to the biotic response. As a consequence, RDA depicted  
24 a general pattern that was not independent of environmental drivers, but it did not allow to  
25 point out the most relevant among the latter.

1 The partition of the resting stage assemblages obtained from the MRT and the environmental  
2 variables that were selected to define its splits provided additional insights that were  
3 consistent with the results of the RDA. Interpreting the role of the environmental variables  
4 that were selected at MRT as causal was certainly tempting, but such an assumption could  
5 prove to be misleading. In fact, environmental variables played a role that was only based on  
6 similarities between their spatial distribution and the spatial distribution of the target, which  
7 in the case of this MRT was the overall structure of the resting stage assemblages, as  
8 described by Euclidean distances between log-transformed lists of taxa. In practice, when a  
9 MRT is trained, a variable is selected at a given split if the “shape” of a suitable threshold in  
10 its spatial distribution matches the best partition of the biotic data (sub)set.

11 Although average SST and depth may not be causally linked to the structure of the resting  
12 stage assemblages, the partition they defined was actually more effective than the one based  
13 on geographical distribution only. As for average SST, it probably does not play a direct role  
14 in the accumulation of resting stages on the sea floor, but it certainly makes sampling stations  
15 in North and Central Adriatic Sea different from all others, with the only exception of a  
16 slightly warmer region roughly corresponding to the Mid Adriatic Pit, which unfortunately  
17 was not sampled. However, North and Central Adriatic waters are not only cooler, but also  
18 very shallow and under the effects of intense terrestrial inputs, as river discharge accounts for  
19 an average input of  $2500 \text{ m}^3 \text{ s}^{-1}$  of fresh water, i.e. more than 30% of the overall river  
20 discharge in the Mediterranean Sea (Struglia et al. 2004).

21 While a small difference in average SST can hardly be a sufficient cause for large scale  
22 ecological effects, extreme events, which are not rare in shallow coastal waters under the  
23 effects of point and diffuse terrestrial run-off, may have occasionally played such a causal  
24 role. As a matter of fact, the SST range in Central and especially in Northern Adriatic Sea is  
25 the second widest in the Mediterranean Sea, after the Black Sea (Shaltout & Omstedt 2014),



1 and extreme events, with SST well below 10 °C and sometimes as low as 7-8 °C are not rare  
2 in coastal regions. As for depth, which was the second explanatory variable selected by the  
3 MRT, causality in driving the composition of resting stage assemblages can be reasonably  
4 excluded. Nevertheless, depth it is not independent of distance from the coastline, which in  
5 turn is related, for instance, to nutrient availability and phytoplankton biomass, which may  
6 have played a role in the accumulation of phytoplankton resting stages. While the latter  
7 explanatory variables were available to the MRT, they were not selected, and this obviously  
8 means that their effects were mediated by more complex relationships, which remain to be  
9 explored.

10 However, the partition obtained from the MRT was significantly more effective than the one  
11 based on a strictly geographical criterion, thus showing that average SST and depth played a  
12 role, independently of the causal or correlational nature of the relationships that link them to  
13 the resting stage assemblages. As we opted for the most parsimonious MRT, only two  
14 explanatory variables were selected. In case more resting stage samples will become  
15 available in the future, a larger data set would most probably allow to train a more complex  
16 MRT and to get deeper insights into distribution and structure of phytoplankton resting stage  
17 assemblages.

18

## 19 **5. CONCLUSIONS**

20 In conclusion, the structure of a resting stage assemblage is obviously not independent of  
21 those of all the phytoplankton assemblages that in time and space contributed to its  
22 formation. In fact, a resting stage assemblage can be regarded as the time- and space-  
23 integrated response of a subset of species to the environmental conditions, including the  
24 physical oceanographic dynamics that favored or prevented sedimentation of the resting  
25 stages. Therefore, this peculiar diachronic assemblage can be regarded as the integral of the

1 biotic responses to seasonal changes and to all the other modifications of the environmental  
2 conditions of the water column, thus summarizing complex time series. A resting stage  
3 assemblage cannot entirely preserve the relevant information in the time series from which it  
4 has been generated, but it can be a very valuable target for one-off sampling activities or  
5 when water column sampling cannot be repeated with a frequency that is as high as to resolve  
6 the complexity of the temporal evolution of phytoplankton assemblages. As sampling of  
7 resting stages can be carried out at very low frequency while preserving the possibility of an  
8 effective comparison between phytoplankton assemblages, it can be also regarded as a very  
9 strong candidate for large scale monitoring of the effects of climate change.

10

11

12 **Acknowledgements.** This study was funded by the monitoring project on the Marine  
13 Strategy Framework Directive operated by Italian CNR and Conisma. We 'd like to thank  
14 Prof. Cesare Corselli, Prof. Daniela Basso, Dr. Eleonora Valbi, Dr. Valentina Bracchi and Dr.  
15 Fabio Marchese for the activity of sampling on board of the CNR scientific vessel. We 'd like  
16 to thank the Reviewers for helping to improve the manuscript.

**1 LITERATURE CITED**

- 2 Abrantes F, Lopes C, Mix A, Pias N (2007) Diatoms in Southeast Pacific surface sediments  
3 reflect environmental properties. *Quat. Sci. Rev.* 26: 155–169
- 4 Adachi M, Sako Y, Ishida, Y (1994) Restriction fragment length polymorphism of ribosomal  
5 DNA internal transcribed spacer and 5.8S regions in Japanese *Alexandrium* species  
6 (Dinophyceae). *J Phycol* 30: 857–863
- 7 Amato A, Orsini L, D’Alelio D, Montresor M (2005) Life cycle, size reduction patterns, and  
8 ultrastructure of the pennate planktonic diatom *Pseudo-nitzschia delicatissima*  
9 (Bacillariophyceae). *J Phycol* 41: 542–556
- 10 Amoroso RO, Pitcher CR, Rijnsdorp AD, McConnaughey RA and others (2018) Bottom  
11 trawl-fishing footprints on the world’s continental shelves. *Proc Natl Acad Sci USA*  
12 115: 10275-10282
- 13 Anderson DM, Lively JJ, Reardon EM, Price CA (1985) Sinking characteristics of  
14 dinoflagellate cysts. *Limnol Oceanogr* 30: 1000-1009
- 15 Anderson DM, Rengefors K (2006) Community assembly and seasonal succession of marine  
16 dinoflagellates in a temperate estuary: The importance of life cycle events. *Limnol*  
17 *Oceanogr* 51: 860-873
- 18 Anglés S, Garces E, Jordi A, Basterretxea G, Palanques A (2010) *Alexandrium minutum*  
19 resting cyst distribution dynamics in a confined site. *Deep-Sea Res II* 57: 210–221
- 20 Ayata SD, Irisson JO, Aubert A, Berline L, Dutay JC, Mayot N, Nieblas AE, D’Ortenzio F,  
21 Palmiéri J, Reygondeau G, Rossi, V, Guieu C (2018) Regionalisation of the  
22 Mediterranean basin, a MERMEX synthesis. *Prog Oceanogr* 163: 7-20
- 23 Barton AD, Pershing AJ, Litchman E, Record NR, Edwards KF and others (2013) The  
24 biogeography of marine plankton traits. *Ecol Lett* 16: 522–34

- 1 Bastianini M, Totti C, Penna A, De Lazzari A, Montresor M (2016) Dinoflagellate cyst  
2 production in the north-western Adriatic Sea. *Mediterr Mar Sci* 17: 751-765
- 3 Bolch CJS (1997) The use of sodium polytungstate for the separation and concentration of  
4 living dinoflagellate cysts from marine sediments. *Phycologia* 36: 472–478
- 5 Bolch CJS, de Salas M (2007) A review of the molecular evidence for ballast water  
6 introduction of the toxic dinoflagellates *Gymnodinium catenatum* and *Alexandrium*  
7 “*tamarensis* complex” to Australia. *Harmful Algae* 6: 465–485
- 8 Breiman L, Friedman JH, Olshen RA, Stone CG (1984) Classification and regression trees.  
9 Wadsworth International Group, Belmont, California
- 10 Bringué M, Thunell RC, Pospelova V, Pinckney JL, Romero OE, Tappa EJ (2018) Physico-  
11 chemical and biological factors influencing dinoflagellate cyst production in the  
12 Cariaco Basin. *Biogeosciences* 15: 2325-2348
- 13 Calbet A (2008) The trophic roles of microzooplankton in marine systems. *ICES J Mar Sci*  
14 65: 325-331
- 15 Casabianca S, Capellacci S, Giacobbe MG, Dell’Aversano C, Tartaglione L, Varriale F,  
16 Narizzano R, Risso F, Moretto P, Dagnino A, Bertolotto R, Barbone E, Ungaro N,  
17 Penna A (2019) Plastic-associated harmful microalgal assemblages in marine. *Environ*  
18 *Pollut* 244: 617–626
- 19 Casabianca S, Casabianca A, Riobó P, Franco JM, Vila M, Penna A (2013) Quantification of  
20 the Toxic Dinoflagellate *Ostreopsis* spp. by qPCR Assay in Marine Aerosol. *Environ*  
21 *Sci Technol* 47: 3788-3795
- 22 Casabianca S, Perini F, Casabianca A, Battocchi C, Giussani V, Chiantore M, Penna A  
23 (2014) Monitoring of toxic *Ostreopsis* cf. *ovata* in recreational waters using qPCR  
24 based assay. *Mar Pollut Bull* 88: 102-109

- 1 Clarke KR (1993) Non-parametric multivariate analyses of changes in community structure.  
2 Aust J Ecol 18: 117-143
- 3 D'Ortenzio F, Ribera d'Alcalà M (2009) On the trophic regimes of the Mediterranean Sea: a  
4 satellite analysis. Biogeosciences 6: 139–148
- 5 De'ath G (2002) Multivariate regression trees: a new technique for modeling species-  
6 environment relationships. Ecology 83: 1105-1117
- 7 De'ath G (2014) mvpart: Multivariate partitioning. R package version 1.6-2.  
8 <https://CRAN.R-project.org/package=mvpart>
- 9 Eigaard OR, Bastardie F, Niels T, Hintzen T, Buhl-Mortensen L, Buhl-Mortensen M and  
10 others (2017) The footprint of bottom trawling in European waters: distribution,  
11 intensity, and seabed integrity. ICES J Mar Sci 74: 847–865
- 12 Ellegaard M, Ribeiro S (2018) The long-term persistence of phytoplankton resting stages in  
13 aquatic 'seed banks'. Biol Rev 93: 166-183
- 14 EMODNet Hydrography Portal (2013) Bathymetric metadata and Digital Terrain Model data  
15 products. <http://www.emodnet-bathymetry.eu>
- 16 Figueroa RI, Bravo I (2005) Sexual reproduction and two different encystment strategies of  
17 *Lingulodinium polyedrum* (Dinophyceae) in culture. J Phycol 41: 370-379
- 18 Finkel ZV, Beardall J, Flynn KJ, Quigg A, Rees TAV, Raven JA (2010) Phytoplankton in a  
19 changing world: cell size and elemental stoichiometry. J Plankton Res 32: 119–137
- 20 Fitzpatrick E, Caron DA, Schnetzer A (2010) Development and environmental application of  
21 a genus-specific quantitative PCR approach for *Pseudo-nitzschia* species. Mar Biol  
22 157: 1161–1169
- 23 French FW, Hargraves PE (1980) Physiological characteristics of plankton diatom resting  
24 spores. Marine Biology Letters 1: 185–195.

- 1 Godhe A, Asplund ME, Härnström K, Saravanan V, Tyagi A, Karunasagar I (2008)  
2 Quantification of diatom and dinoflagellate biomasses in coastal marine seawater  
3 samples by real-time PCR. *Appl Environ Microbiol* 74: 7174-7182
- 4 Gong W, Marchetti A (2019) Estimation of 18S Gene Copy Number in Marine Eukaryotic  
5 Plankton Using a Next-Generation Sequencing Approach. *Front Mar Sci* 6: 219
- 6 Gottschling M, Knop R, Plötner J, Kirsch M, Willems H, Keupp H, (2005) A molecular  
7 phylogeny of *Scrippsiella sensu lato* (Calciodinellaceae, Dinophyta) with  
8 interpretations on morphology and distribution. *Eur J Phycol* 40: 207-220
- 9 Guillard RRL (1975) Culture of phytoplankton for feeding marine invertebrates. In: Smith  
10 WL, Chanley MH (eds) *Culture of Marine Invertebrate Animals*. Plenum Press, p 26–  
11 60
- 12 Hallegraeff GM (2010) Ocean climate change, phytoplankton community responses, and  
13 harmful algal blooms: a formidable predictive challenge. *J Phycol* 46: 220-235
- 14 Halpern BS, Walbridge S, Selkoe KA, Kappel CV, Micheli F, D'Agrosa C and others (2008)  
15 A global map of human impact on marine ecosystems. *Science* 319: 948-952
- 16 Hammer Ø, Harper D.A.T, PD Ryan (2001) PAST: Paleontological Statistics Software  
17 Package for Education and Data Analysis. *Palaeontol. electron* 4: 9 pp
- 18 Harland R., Nordberg K, LFilipsson H (2004) The seasonal occurrence of dinoflagellate cysts  
19 in surface sediments from Koljö Fjord, west coast of Sweden – a note. *Rev Palaeobot*  
20 *Palynology* 128:107-117
- 21 Hernández-Fariñas T, Soudant D, Barillé L, Belin C, Lefebvre A, Bacher C (2014) Temporal  
22 changes in the phytoplankton community along the French coast of the eastern English  
23 Channel and the southern Bight of the North Sea. *ICES J Mar Sci* 71: 821-833

- 1 Hubbard KA, Olson CH, Armbrust EV (2014) Molecular characterization of *Pseudo-*  
2 *nitzschia* community structure and species ecology in a hydrographically complex  
3 estuarine system (Puget Sound, Washington, USA). *Mar Ecol Prog Ser* 507: 39–55
- 4 Huertas IE, Rouco M, López-Rodas V, Costas E (2011) Warming will affect phytoplankton  
5 differently: evidence through a mechanistic approach. *Proc R Soc B* 278: 3534-3543
- 6 Kim JH, Kim JH, Wang P, Park BS, Han MS (2016) An improved quantitative real-time PCR  
7 assay for the enumeration of *Heterosigma akashiwo* (Raphidophyceae) cysts using a  
8 DNA debris removal method and a cyst-based standard curve. *PLoS One* 11: 1-17
- 9 Kon NF, Lau WLS, Hii KS, Law IK, Teng ST, Lim HC, Takahashi K, Gu HF, Lim PT, Leaw  
10 CP (2017) Quantitative real-time PCR detection of a harmful unarmoured  
11 dinoflagellate, *Karlodinium australe* (Dinophyceae). *Phycol Res* 65: 291-298
- 12 Kremp A, Oja J, LeTortorec AH, Hakanen P, Tahvanainen P, Tuimala J, Suikkanen S (2016)  
13 Diverse seed banks favour adaptations of microalgal populations to future climate  
14 conditions. *Environ Microbiol* 18: 679–691
- 15 Kremp A, Rengefors K, Montresor M (2009) Species-specific encystment patterns in three  
16 Baltic cold-water dinoflagellates: the role of multiple cues in resting cyst formation.  
17 *Limnol Oceanogr* 54: 1125–1138
- 18 Kuwata A, Hama T, Takahashi M (1993) Ecophysiological characterization of two life forms,  
19 resting spores and resting cells, of a marine planktonic diatom, *Chaetoceros*  
20 *pseudocurvisetus*, formed under nutrient depletion. *Mar Ecol Prog Ser* 102: 245-255
- 21 Larkin M, Blackshields G, Brown N, Chenna R, McGettigan P, McWilliam H, Valentin F,  
22 Wallace I, Wilm A, Lopez R, Thompson JD, Gibson TJ, Higging DG (2007) Clustal W  
23 and Clustal X version 2.0. *Bioinformatics* 23: 2947–2948

- 1 Lee SY, Jeong HJ, You JH, Kim SJ (2018) Morphological and genetic characterization and  
2 the nationwide distribution of the phototrophic dinoflagellate *Scrippsiella lachrymosa*  
3 in the Korean waters. *Algae* 33: 21-35
- 4 Lelong A, Hégaret H, Soudant P, Bates SS (2012) *Pseudo-nitzschia* (Bacillariophyceae)  
5 species, domoic acid and amnesic shellfish poisoning: revisiting previous paradigms.  
6 *Phycologia* 51: 168–216
- 7 Lennon JT, Jones SE (2011) Microbial seed banks: the ecological and evolutionary  
8 implications of dormancy. *Nat Rev Microbiol* 9: 119–130
- 9 Ludwig W, Dumont E, Meybeck M, Heussner S (2009) River discharges of water and  
10 nutrients to the Mediterranean and Black Sea: Major drivers for ecosystem changes  
11 during past and future decades? *Prog Oceanogr* 80: 199–217
- 12 Lundholm N, Clarke A, Ellegaard M (2010). A 100-year record of changing *Pseudo-nitzschia*  
13 species in a sill-fjord in Denmark related to nitrogen loading and temperature. *Harmful*  
14 *Algae* 9: 449-457
- 15 Lundholm N, Ribeiro S, Andersen TJ, Koch T, Godhe A, Ekelund F, Ellegaard M (2011)  
16 Buried alive – germination of up to a century-old marine protist resting stages.  
17 *Phycologia* 50: 629–640
- 18 McQuoid M, Godhe A (2004) Recruitment of coastal planktonic diatoms from benthic versus  
19 pelagic cells: Variations in bloom development and species composition. *Limnol*  
20 *Oceanogr* 49: 1123-1133
- 21 Montresor M, Di Prisco C, Sarno D, Margiotta F, Zingone A (2013) Diversity and  
22 germination patterns of diatom resting stages at a coastal Mediterranean site. *Mar Ecol*  
23 *Prog Ser* 484: 79–95
- 24 Mutshinda CM, Finkel ZV, Widdicombe CE, Irwin AJ (2016) Ecological equivalence of  
25 species within phytoplankton functional groups. *Funct Ecol* 30: 1714-1722



- 1 Oksanen J, Blanchet FG, Friendly M, Kindt R, Legendre P, McGlinn D, Minchin PR, O'Hara  
2 RB, Simpson GL, Solymos P, Stevens HMH, Szoecs E, Wagner H (2018) Vegan:  
3 Community Ecology Package. R package ver 2.5-3. [https://CRAN.R-](https://CRAN.R-project.org/package=vegan)  
4 [project.org/package=vegan](https://CRAN.R-project.org/package=vegan)
- 5 Orlova TY, Morozova TV (2009) Resting stages of microalgae in recent marine sediments of  
6 Peter the Great Bay, Sea of Japan. *Russian Journal of Marine Biology* 35: 313–322
- 7 Otero J, Bode A, Álvarez-Salgado XA, Varela M (2018) Role of functional traits variability  
8 in the response of individual phytoplankton species to changing environmental  
9 conditions in a coastal upwelling zone. *Mar Ecol Prog Ser* 2018: 33–47
- 10 Parsons ML, Dortch Q (2002) Sedimentological evidence of an increase in *Pseudo-nitzschia*  
11 (Bacillariophyceae) abundance in response to coastal eutrophication. *Limnol.*  
12 *Oceanogr.* 47: 551–558
- 13 Penna A, Battocchi B, Garcés E, Anglès S, Cucchiari E, Totti C, Kremp A, Satta C, Giacobbe  
14 MG, Bravo I, Bastianini M (2010) Detection of microalgal resting cysts in European  
15 coastal sediments using a PCR-based assay. *Deep-Sea Res. Part II-Top. Stud.*  
16 *Oceanogr.* 57: 288-300
- 17 Penna A, Bertozzini E, Battocchi C, Galluzzi L, Giacobbe MG, Vila M, Garcés E, Luglié A,  
18 Magnani M (2007) Monitoring of HAB species in the Mediterranean Sea through  
19 molecular methods. *J Plankton Res* 29: 19-38
- 20 Penna A, Casabianca S, Guerra AF, Vernesi C, Scardi M (2017) Analysis of phytoplankton  
21 assemblage structure in the Mediterranean Sea based on high-throughput sequencing of  
22 partial 18S rRNA sequences. *Mar Genom* 36: 49-55
- 23 Penna A, Casabianca S, Perini F, Bastianini M, Riccardi E, Pigozzi S, Scardi M (2013) Toxic  
24 *Pseudo-nitzschia* spp. in the northwestern Adriatic Sea: characterization of species

- 1 composition by genetic and molecular quantitative analyses. J Plankton Res 35: 352–  
2 366
- 3 Penna A, Galluzzi L (2013) The quantitative real-time PCR applications in the monitoring of  
4 marine harmful algal bloom (HAB) species. Environ Sci Pollut Res 20: 6851-6862
- 5 Perini F, Bastianini M, Capellacci S, Pugliese L, Dipoi E, Cabrini M, Buratti S, Marini M,  
6 Penna A (2019) Molecular methods for cost-efficient monitoring of HAB (harmful  
7 algal bloom) dinoflagellate resting cysts. Mar Pollut Bull 147: 209–218
- 8 Perini F, Casabianca A, Battocchi C, Accoroni S, Totti C, Penna A (2011) New Approach  
9 Using the Real-Time PCR Method for Estimation of the Toxic Marine Dinoflagellate  
10 *Ostreopsis cf. ovata* in Marine Environment. PLoS ONE 6(3): e17699.
- 11 Piredda R, Sarno D, Lange CB, Tomasino MP, Zingone A, Montresor M (2017) Diatom  
12 resting stages in surface sediments: a pilot study comparing Next Generation  
13 Sequencing and Serial Dilution Cultures. Cryptogam. Algal. 38: 31-46
- 14 Pugliese L, Casabianca S, Perini F, Andreoni F, Penna A (2017) A high resolution melting  
15 method for the molecular identification of the potentially toxic diatom *Pseudo-nitzschia*  
16 spp. in the Mediterranean Sea. Sci Rep 7: 4259
- 17 QGIS Development Team (2015) QGIS Geographic Information System. Open Source  
18 Geospatial Foundation Project <http://qgis.osgeo.org>
- 19 R Core Team (2018) R: A language and environment for statistical computing. R Foundation  
20 for Statistical Computing, Vienna, Austria. <https://www.R-project.org/>
- 21 Radzikowski J (2013) Resistance of dormant stages of planktonic invertebrates to adverse  
22 environmental conditions. J Plankton Res 35: 707–723
- 23 Rao CR (1964) The Use and Interpretation of Principal Component Analysis in Applied  
24 Research. Sankhyā: The Indian Journal of Statistics, Series A (1961-2002) 26: 329-358

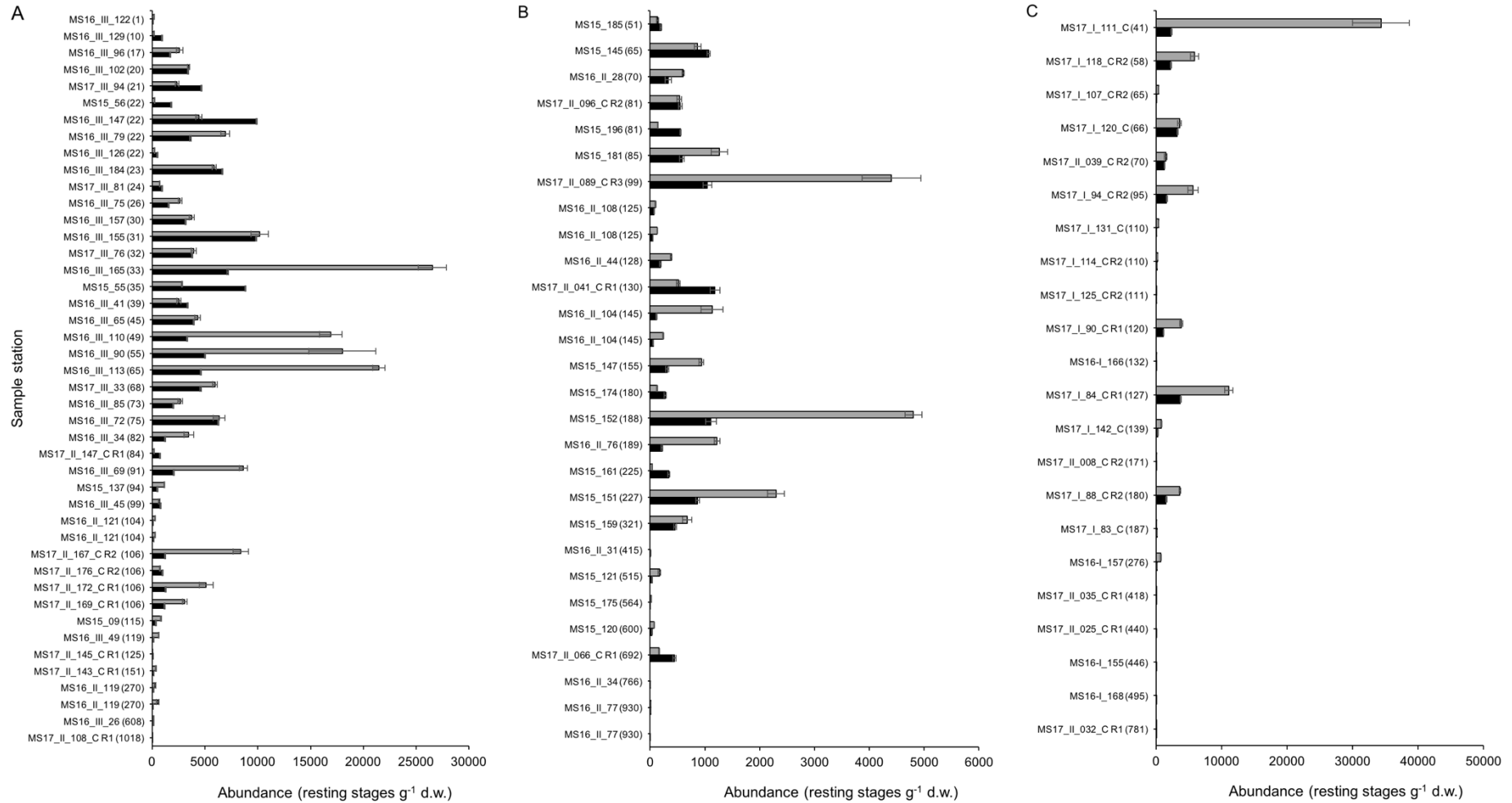
- 1 Reygondeau G, Guieu C, Benedetti F, Irisson JO, Ayata SD, Gasparini S, Koubbi P (2017)  
2 Biogeochemical regions of the Mediterranean Sea: an objective multidimensional and  
3 multivariate environmental approach. *Prog Oceanogr* 151: 138-148
- 4 Ribeiro S, Amorim A (2008) Environmental drivers of temporal succession in recent  
5 dinoflagellate cyst assemblages from a coastal site in the North-East Atlantic (Lisbon  
6 Bay, Portugal). *Mar Micropaleontol* 68: 156-178
- 7 Rubino F, Saracino OD, Moscatello S, Belmonte G (2009) An integrated water/sediment  
8 approach to study plankton (a case study in the southern Adriatic Sea). *J Mar Syst* 78:  
9 536-546
- 10 Russo T, D'Andrea L, Parisi A, Cataudella S (2014) VMSbase: An R-Package for VMS and  
11 Logbook Data Management and Analysis in Fisheries Ecology. *PLoS One* 9(6):  
12 e100195
- 13 Russo T, D'Andrea L, Parisi A, Martinelli M, Belardinelli A, Boccoli F, Cignini I, Tordoni  
14 M, Cataudella S (2016) Assessing the fishing footprint using data integrated from  
15 different tracking devices: issues and opportunities. *Ecol Indic* 69: 818–827
- 16 Satta C, Anglès S, Garcés E, Lugliè A, Padedda BM, Sechi N (2010) Dinoflagellate cysts in  
17 recent sediments from two semi-enclosed areas of the Western Mediterranean Sea  
18 subject to high human impact. *Deep-Sea Res. Part II-Top. Stud. Oceanogr.* 57: 256-267
- 19 Scholin CA, Herzog, M, Sogin, M, Anderson D. M. (1994) Identification of group and strain-  
20 specific using genetic markers from globally distributed *Alexandrium* (Dinophyceae).  
21 II. Sequence analysis of fragments of the LSU rRNA gene. *J Phycol* 30: 999–1011
- 22 Shaltout M, Omstedt A (2014) Recent sea surface temperature trends and future scenarios for  
23 the Mediterranean Sea. *Oceanologia* 56: 411-443
- 24 Shanks AL, Trent JD (1980) Marine snow: sinking rates and potential role in vertical flux.  
25 *Deep Sea Research Part A, Oceanographic Research Papers*, 27: 137-143

- 1 Struglia MV, Mariotti A, Filograsso A (2004) River discharge into the Mediterranean Sea:  
2 climatology and aspects of the observed variability. *J Clim* 17: 4740-4751
- 3 Taylor FJR (1987) The biology of dinoflagellates. In: Taylor FJR (ed) The biology of  
4 dinoflagellates. Blackwell Scientific, Oxford.
- 5 Valbi E, Ricci F, Capellacci S, Casabianca S, Scardi M, Penna A (2019) A model predicting  
6 the PSP toxic dinoflagellate *Alexandrium minutum* occurrence in the coastal waters of  
7 the NW Adriatic Sea. *Sci Rep* 9: 4166
- 8 Wollenberg AL (1977) Redundancy analysis. An alternative for canonical correlation  
9 analysis. *Psychometrika* 42: 207-219
- 10 Ye J, Coulouris G, Zaretskaya I, Cutcutache I, Rozen S, Madden TL (2012) Primer-BLAST:  
11 a tool to design target-specific primers for polymerase chain reaction. *BMC*  
12 *Bioinformatics* 13: 134
- 13 Yuan J, Li M, Lin S (2015) An Improved DNA Extraction Method for Efficient and  
14 Quantitative Recovery of Phytoplankton Diversity in Natural Assemblages. *PLoS One*  
15 10 (7): e0133060
- 16 Zhang Y, Lu S, Zhang C, Gao Y (2010). Distribution and germination of viable diatom  
17 resting stage cells in sediments of the East China Sea. *Acta Oceanol Sin* 29: 121–128  
18

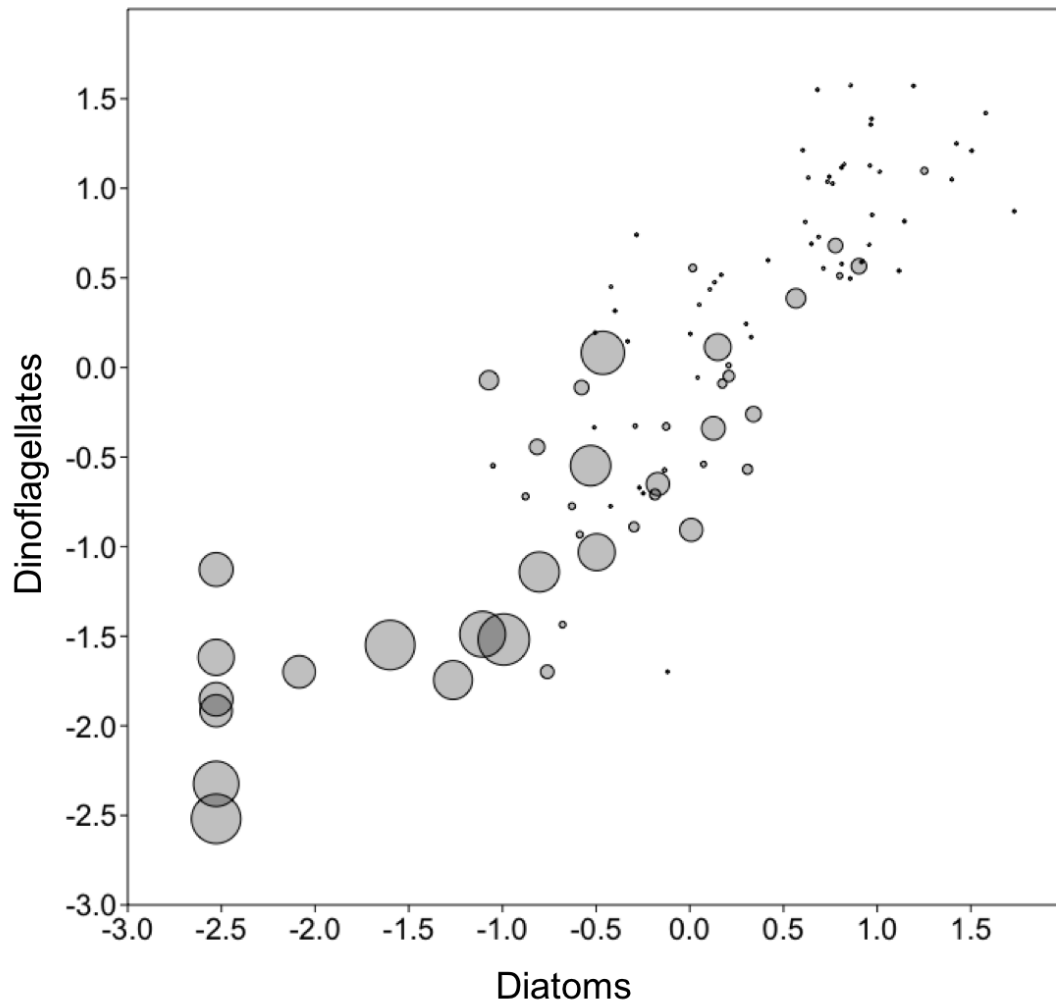
1 Table 1. SIMPER analysis of the three assemblages of resting stages defined by the Multivariate Regression Tree (Fig. 4). From left to right:  
 2 name and short name of the taxon, average Euclidean distance, percentage contribution to the overall Euclidean distance, cumulative percentage  
 3 contribution to the overall Euclidean distance and average log-transformed abundance in each leaf of the Multivariate Regression Tree (both bars  
 4 and numerical values are shown).

Taxon	Short name	Average D	% D	Total % D	● Temp < 18.57°C	▲ Temp ≥ 18.57° Depth < 368 m	□ Temp ≥ 18.57° Depth ≥ 368 m
Diatom spores	Diat	3.304	15.610	15.61	3.50	2.84	0.97
<i>Alexandrium minutum</i> cysts	Amin	2.735	12.920	28.53	2.03	0.42	0.00
<i>Ditylum brightwellii</i> spores	Dity	2.433	11.490	40.02	1.64	0.22	0.00
Dinoflagellate cysts	Dint	2.307	10.900	50.92	3.45	2.52	1.25
<i>Skeletonema</i> spp. spores	Skel	1.689	7.981	58.90	1.46	0.08	0.00
<i>Thalassiosira</i> spp. spores	Thal	1.685	7.959	66.86	1.56	0.59	0.10
<i>Protoceratium reticulatum</i> cysts	Prot	1.555	7.348	74.21	1.50	0.46	0.06
<i>Chaetoceros socialis</i> spores	Chae	1.332	6.295	80.50	0.97	0.43	0.47
<i>Gymnodinium</i> spp. cysts	Gymn	1.296	6.122	86.63	1.73	1.09	0.12
<i>Gonyaulax spinifera</i> cysts	Gspi	0.956	4.517	91.14	0.99	0.10	0.10
<i>Pseudo-nitzschia</i> spp. spores	Pseu	0.916	4.325	95.47	1.05	0.67	0.04
<i>Lingulodinium polyedrum</i> cysts	Ling	0.641	3.028	98.50	1.01	0.31	0.10
<i>Scrippsiella trochoidea</i> complex cysts	Scri	0.199	0.938	99.43	0.63	0.28	0.08
<i>Alexandrium tamarense/mediterraneum</i> cysts	Atam	0.091	0.432	99.87	0.21	0.09	0.02
<i>Heterosigma akashiwo</i> cysts	Hets	0.015	0.069	99.94	0.00	0.02	0.00
<i>Alexandrium pacificum</i> cysts	Apac	0.011	0.050	99.99	0.01	0.03	0.00
<i>Heterocapsa triquetra</i> cysts	Hetc	0.003	0.014	100.00	0.00	0.01	0.00

The above values are  $\log_{10}(x+1)$  cysts/spores  $g^{-1}$  DW sediment



1  
2 Figure 1. Abundance of resting stages of Dinophyceae (black columns) and Bacillariophyceae (grey columns) expressed as number of resting  
3 stages  $g^{-1}$  d.w. of sediment determined by qPCR assay in the Mediterranean Sea. Samples on y axis are in order of depth from the less deep to  
4 the deepest, the depth, expressed in meters below sea level is reported in brackets. A, Adriatic Sea; B, Ionian Sea; C, Tyrrhenian Sea.



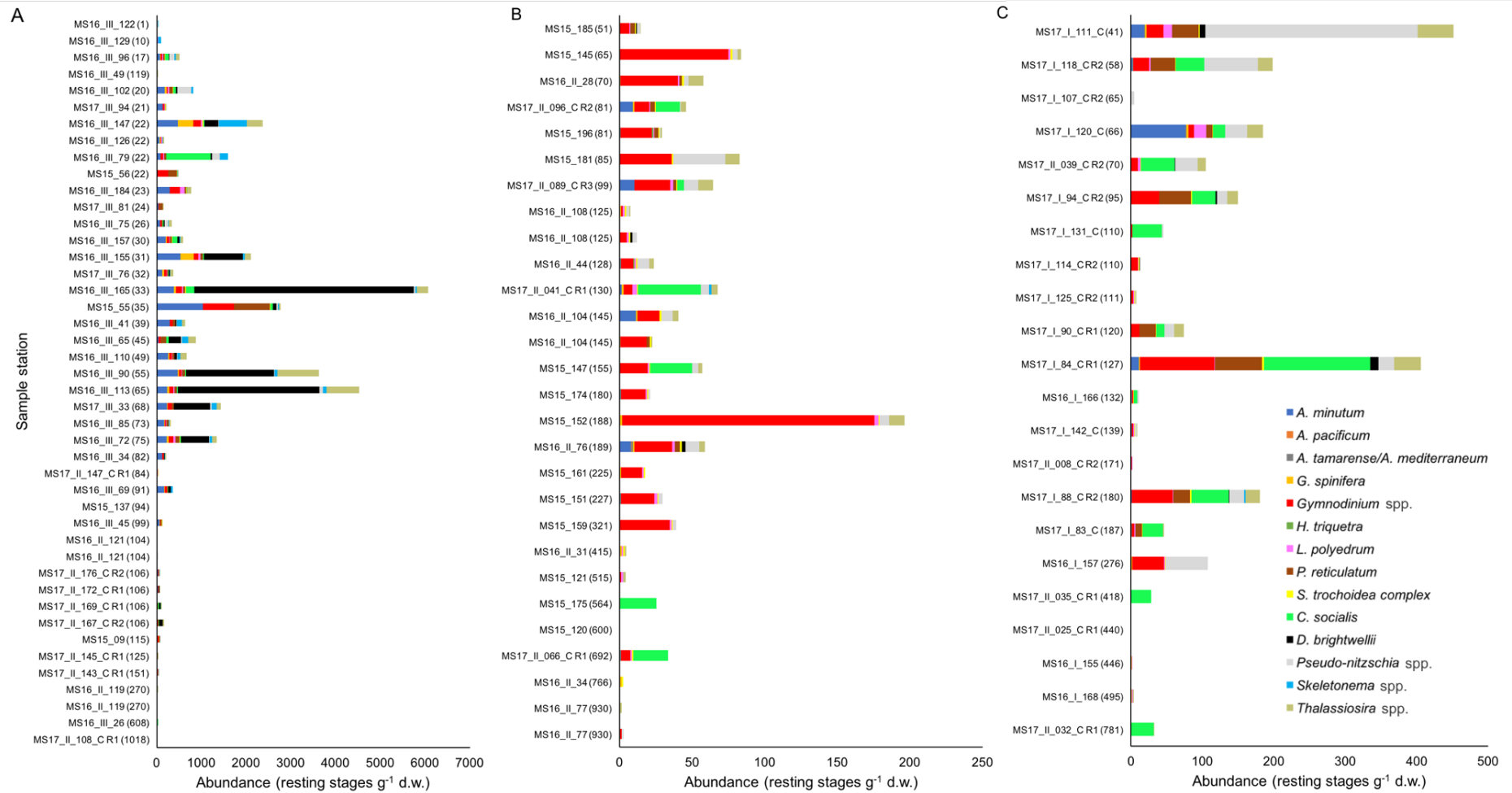
1

2 Figure 2. Total abundance of dinoflagellates vs. diatoms, expressed as resting stages  $\text{g}^{-1}$  d.w.  
3 of sediment by qPCR based assay. Resting stage abundances were log-transformed as  $x' =$   
4  $\log_{10}(x+1)$ . Circle size is proportional to depth. While covariation in dinoflagellate and  
5 diatom abundances emerges as the main pattern, smaller circles, corresponding to shallower  
6 samples, are mostly associated to higher abundances.

7

8

9

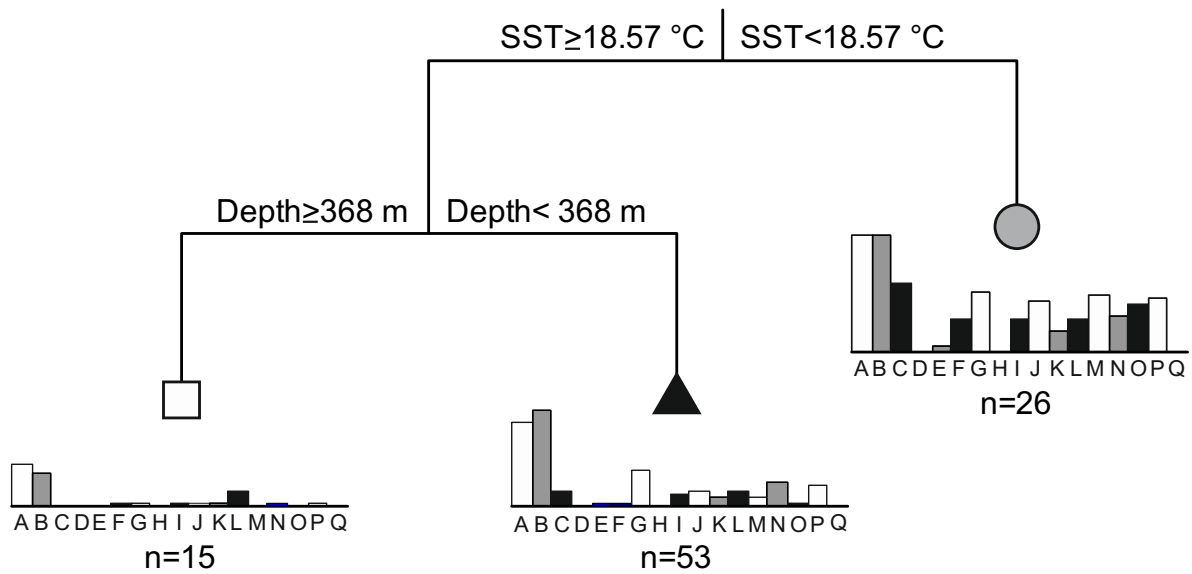


- 1 Figure 3. Resting stages abundance expressed as number of resting stages  $g^{-1}$  d.w. of sediment determined by qPCR assay in the Mediterranean
- 2 Sea. Among all resting stage taxa abundance, target toxic producing taxa were also shown (i.e. *A. minutum*, *A. pacificum*, *G. spinifera*, *L.*



- 1 *polyedrum*, *P. reticulatum*, *Pseudo-nitzschia* spp.). Samples on y axis are in order of depth from the less deep to the deepest, the depth,
- 2 expressed in meters below sea level is reported in brackets. A, Adriatic Sea; B, Ionian Sea; C, Tyrrhenian Sea.

1



2

3

4 Figure 4. Multivariate Regression Tree. The most parsimonious optimum structure, with

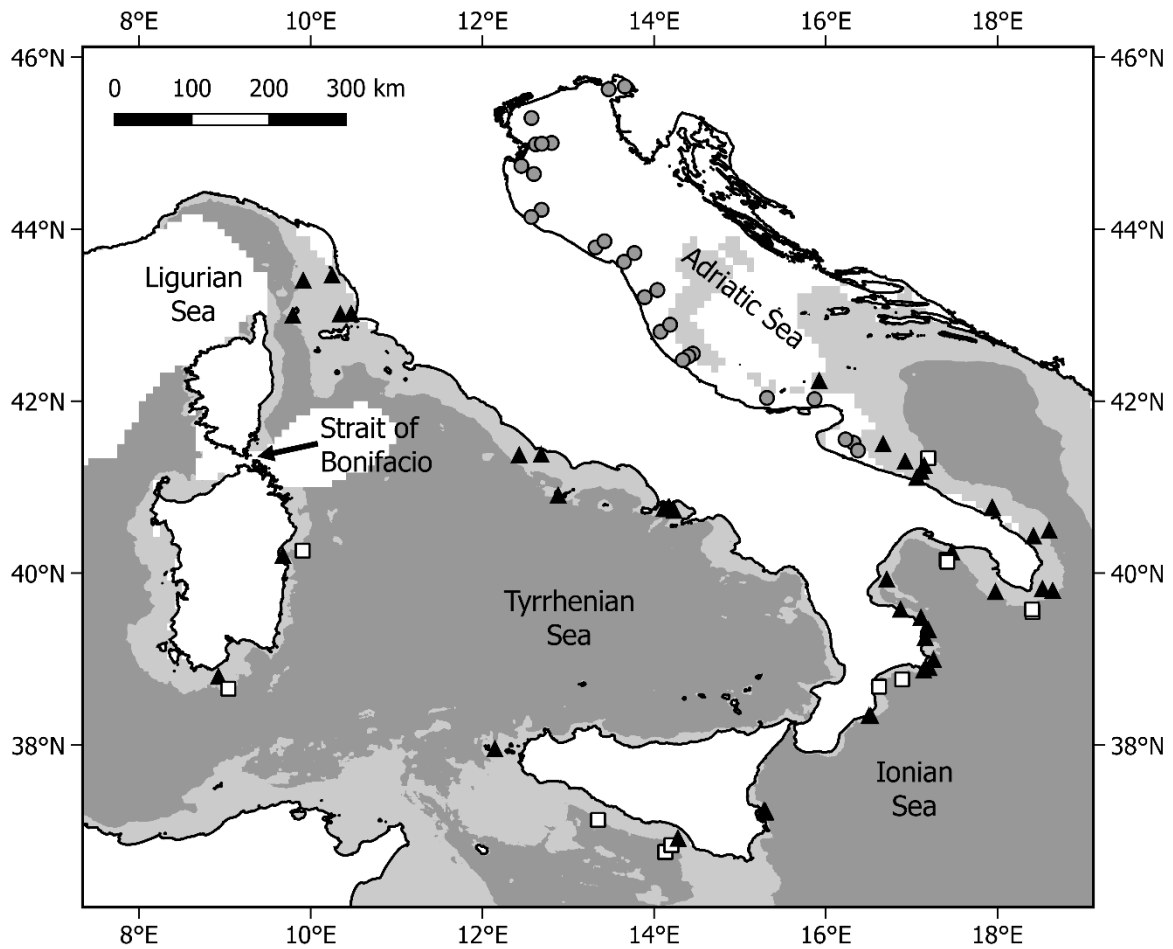
5 three leaves only, was selected according to the cross-validation relative error plot (Fig. S2).

6 The average assemblage structure is shown at each leaf by a bar plot. Abundances are log-

7 transformed and taxa are shown by letters: dinoflagellate cysts (A), diatom spores (B), *A.*8 *minutum* cysts (C), *A. pacificum* cysts (D), *A. tamarense/mediterraneum* cysts (E), *G.*9 *spinifera* cysts (F), *Gymnodinium* spp. cysts (G), *H. triquetra* cysts (H), *L. polyedrum* cysts10 (I), *P. reticulatum* cysts (J), *S. trochoidea* complex cysts (K), *C. socialis* spores (L), *D.*11 *brightwellii* spores (M), *Pseudo-nitzschia* spp. non-viable dormant stages (N), *Skeletonema*12 spp. spores (O), *Thalassiosira* spp. spores (P), *H. akashiwo* cysts (Q).

13

1



2

3 Figure 5. The three different shades of gray show the regions corresponding to the  
 4 assemblage structures obtained from the MRT. Sampling stations in each region are  
 5 associated to the same symbols as in Table 1 and Fig. 4. High resting stage densities were  
 6 found at colder stations in North and Central Adriatic Sea (gray circles on white),  
 7 intermediate densities at warmer and shallower stations along the coastline of all the other  
 8 basins (black triangles on light gray) and low density, with reduced species richness, at  
 9 warmer and deeper stations (white squares on dark gray).